

MIP-BASED INSTANTANEOUS CONTROL OF MIXED-INTEGER PDE-CONSTRAINED GAS TRANSPORT PROBLEMS

MARTIN GUGAT¹, GÜNTER LEUGERING¹, ALEXANDER MARTIN²,
MARTIN SCHMIDT^{2,3}, MATHIAS SIRVENT², DAVID WINTERGERST¹

ABSTRACT. We study the transient optimization of gas transport networks including both discrete controls due to switching of controllable elements and nonlinear fluid dynamics that are described by the system of partial differential Euler equations. This combination leads to mixed-integer optimization problems subject to nonlinear hyperbolic partial differential equations on a graph. We propose an instantaneous control approach in which suitable Euler discretizations yield systems of ordinary differential equations on a graph. This networked system of ordinary differential equations is shown to be well-posed and affine-linear solutions of these systems are derived analytically. As a consequence, finite-dimensional mixed-integer linear optimization problems are obtained for every time step that can be solved to global optimality using general-purpose solvers. We illustrate our approach in practice by presenting numerical results on a realistic gas transport network.

1. INTRODUCTION

The mathematical optimization of gas transport networks has been intensively studied during the recent years. There are at least two reasons for this. First, natural gas is important for the energy turnaround in many countries, e.g., in Germany. Thus, it is an important topic in politics and economy. Second, it combines various mathematical challenges that make applied optimization difficult and thus interesting, e.g., discrete decisions due to switching of controllable elements like valves or compressor machines and nonlinear gas physics. The latter is mainly described by the Euler equations that are given by a system of nonlinear hyperbolic partial differential equations (PDEs).

The literature on mathematical optimization of gas networks can be mainly split up along the aspects that make the problems hard to solve. For recent surveys of this field of research see, e.g., [24, 28, 40] and the references therein.

One branch of literature mainly focuses on discrete aspects of the models that are needed for describing discrete controls of devices like (control) valves or compressor machines. Since an accurate model of these discrete controls together with highly detailed physics models typically leads to nonconvex mixed-integer nonlinear problems (MINLPs) that are hard to solve, a lot of research relies on (piecewise) linearization techniques for obtaining mixed-integer linear (MIP) models that can be solved with state-of-the-art MIP solvers; see, e.g., [13–17, 33–37].

Another branch assumes that the discrete controls are externally given and focuses on the nonlinear aspects of the problem. However, even after fixing the discrete decisions, the combination of highly nonlinear gas dynamics in pipes and typically nonlinear as well as nonconvex models of technical entities like, e.g.,

Date: April 11, 2017.

2010 Mathematics Subject Classification. 49J15, 49J20, 76B75, 90C11, 90C35.

Key words and phrases. Mixed-integer optimal control, Instantaneous control, Partial differential equations on graphs, Gas networks, Mixed-integer linear optimization.

compressor machines, from the engineering literature already leads to nonlinear programming (NLP) models that are themselves hard to solve; see, e.g., [45, 46]. Nevertheless, following this approach it is possible to model (more or less) arbitrary finite-dimensional nonlinearities. However, not being able to switch discrete decisions has always been a significant drawback of these approaches. This is the reason why extended nonlinear models of MPEC type have been studied that allow for switching of discrete states within continuous models; see, e.g., [4, 39, 41–44].

Despite the fact that a lot of research solely focuses on one of the above sketched approaches, there has also been some work that tries to combine the nonlinear and the discrete aspects of the problem; see, e.g., [8] or the approaches described in [28]. Recently, (penalty) alternating direction methods have been used to combine mixed-integer and continuous solution strategies in a hybrid approach in [18, 19] and a Benders-like approach for highly challenging transient problems is addressed in [24].

Not all but most of the publications referenced so far deal with the stationary case, i.e., neglect all time-dependent aspects. Of course, research has also been carried out regarding the transient case. Computational studies of NLP solution techniques for fully discretized systems can be found in [9, 10, 47], whereas theoretical studies of controllability, stabilization, or the existence of stationary states of gas flow are topics of [2, 3, 5, 22, 23]. Very recently, an optimal control approach for transient gas network flow without discrete aspects has been studied in [48].

Our contribution is a first step towards the combination of the aspects that have been studied mainly in a separate way, i.e., we study an approach to optimize discrete and continuous controls that are constrained by systems of algebraic nonlinear and hyperbolic partial differential equations on a graph. The optimization of such a system in its full beauty is by far out of reach of today’s algorithmic technology and theoretical knowledge. Our approach builds upon the fact that stationary mixed-integer nonlinear problems can be solved comparably fast, reliable, and accurate with mixed-integer linearization techniques that have been developed in the last years. We exploit these techniques and embed them in an instantaneous control approach. To this end, we discretize the space-time dependent Euler PDE system on a graph in a suitable way that allows us to analytically derive solutions. These solutions then allow to formulate linear models in every time step of the proposed instantaneous control method. Moreover, we show that the linear problems that have to be solved in every time step of our method are well-posed.

Instantaneous control has been used frequently for challenging control problems; see, e.g., [6] for instantaneous control of backward-facing step flows, [1] for the control of linear wave equations, [26] for the control of wave equations in networks, [27] for instantaneous control of vibrating string networks, or [25] for an application to traffic flows. To the best of our knowledge, there is no published research on instantaneous control of mixed-integer optimal control problems with hyperbolic PDEs on graphs.

The remainder of the paper is structured as follows. In Section 2 we introduce the problem under consideration and present the models of gas physics and engineering. Afterward, in Section 3 we discuss the instantaneous control approach. To obtain a fully specified algorithm we also discuss suitable time discretization schemes in order to obtain semi-discretizations of the Euler equations that are tailored for our MIP-based control approach. This is done in Section 4, where we also derive solutions of the semi-discretized systems for which we prove well-posedness in Section 5. In Section 6, we finally present a computational case study to show the capability of our approach for controlling realistic networks. The paper closes with some concluding remarks in Section 7.

2. PROBLEM DESCRIPTION

We consider gas transport networks that we model using a directed graph $G = (V, A)$ with node set V and arc set A . The set of nodes is partitioned into the set of entry nodes V_+ , where gas is supplied, the set of exit nodes V_- , where gas is discharged, and the set of inner nodes V_0 . That means, we have $V = V_+ \cup V_- \cup V_0$. Arcs $a = (u, v) \in A$ belong to different subsets of the arc set A depending on the specific network element that they model. In this paper, we consider pipes A_{pi} , valves A_{vl} , control valves A_{cv} , and compressor machines A_{cm} .

In order to formulate a complete model for the entire network we have to specify some continuity conditions for which we need additional notation for the set of ingoing arcs $\delta^{\text{in}}(u) := \{a \in A : \exists v \in V \text{ with } a = (v, u)\}$ and the set of outgoing arcs $\delta^{\text{out}}(u) := \{a \in A : \exists v \in V \text{ with } a = (u, v)\}$ of a node $u \in V$.

Throughout the paper, we consider a given finite time horizon $[0, \mathcal{T}]$. We now describe the model of every arc and node type mentioned above.

2.1. Pipes. Pipes are used to transport gas through the network. They outnumber all other types of elements. We model pipes as one-dimensional arcs $a = (u, v) \in A_{\text{pi}}$. Gas flow through pipes is modeled by the Euler equations that are given as a system of nonlinear hyperbolic partial differential equations (PDEs), which represent the motion of a compressible non-viscous gas. They consist of the continuity equation, the balance of moments, and the energy equation; see, e.g., [11] and [32].

$$\begin{aligned} \partial_t \rho + \partial_x(\rho v) &= 0, \\ \partial_t(\rho v) + \partial_x(p + \rho v^2) &= -\frac{\lambda}{2D} \rho v |v| - g \rho h', \\ \partial_t \left(\rho \left(\frac{1}{2} v^2 + e \right) \right) + \partial_x \left(\rho v \left(\frac{1}{2} v^2 + e \right) + p v \right) &= -\frac{k_w}{D} (T - T_w). \end{aligned} \quad (1)$$

Here, $\rho = \rho(x, t) \in \mathbb{R}_+$ denotes the density, $v = v(x, t) \in \mathbb{R}$ the velocity of the gas, $T = T(x, t) \in \mathbb{R}$ its temperature, and $p = p(x, t) \in \mathbb{R}_+$ its pressure. We further denote with g the gravitational constant, with $h' = h'(x) \in [-1, 1]$ the slope of the pipe (that we assume to be constant), with λ the friction coefficient of the pipe, with D the diameter, with k_w the heat coefficient, with $T_w = T_w(x)$ the temperature of the pipe's wall, and the variable $e = c_v T + gh$ denotes the internal energy, where c_v is the specific heat. In what follows, $x \in [0, L]$ denotes the spatial coordinate and L is the length of the pipe. The conserved, respectively balanced, quantities of the system are the mass flow $q = A \rho v$ (where A is the cross-sectional area of the pipe), the density ρ , and the total energy $E = \rho(1/2 v^2 + e)$. In addition to the Equations (1) we use the constitutive law for a real gas

$$p = R_s \rho T z(p, T), \quad (2)$$

where $z = z(p, T)$ is the real-gas, or compressibility, factor and R_s is the specific gas constant. Note that $z = 1$ holds for ideal gas.

We only consider the isothermal case but note that the temperature may have a significant effect: Long pipes may develop large temperature gradients depending on the weather and flow conditions. In the isothermal case ($T \equiv \text{const}$) the energy equation becomes obsolete. Thus, we obtain

$$\begin{aligned} \partial_t \rho + \partial_x(\rho v) &= 0, \\ \partial_t(\rho v) + \partial_x(p + \rho v^2) &= -\frac{\lambda}{2D} \rho v |v| - g \rho h'. \end{aligned} \quad (3)$$

It is often more convenient to express the state variables in a different way in which the mass flow q and the pressure p in a pipe are used. Under the additional assumption of a constant compressibility factor, i.e., $z(p, T) = z_m$, we have $p = c^2 \rho$

for the pressure. The speed of sound c can then be derived from the constants used in the constitutive law (2) via $c^2 = R_s T z_m$.

With this, we can rewrite System (3) as follows:

$$\begin{aligned}\partial_t p + \frac{c^2}{A} \partial_x q &= 0, \\ \partial_t q + \partial_x \left(A p + \frac{c^2}{A} \frac{q^2}{p} \right) &= -\frac{\lambda c^2}{2DA} \frac{q|q|}{p} - \frac{gA}{c^2} h' p.\end{aligned}$$

For small velocities ($|v| \ll c$) we arrive at the semi-linear model; see [38].

$$\begin{aligned}\partial_t p + \frac{c^2}{A} \partial_x q &= 0, \\ \partial_t q + A \partial_x p &= -\frac{\lambda c^2}{2DA} \frac{q|q|}{p} - \frac{gA}{c^2} h' p.\end{aligned}\tag{4}$$

Finally, we fix the following shorthand notation for pipes $a = (u, v)$. We write $p_{a,u}(t) := p_a(0, t)$ and $p_{a,v}(t) := p_a(L_a, t)$ as well as $q_{a,u}(t) := q_a(0, t)$ and $q_{a,v}(t) := q_a(L_a, t)$ for the pressure and the mass flow, respectively. Moreover, we define bounds for the mass flow variables:

$$q_{a,u}(t), q_{a,v}(t) \in [q_a^-, q_a^+] \quad \text{for all } a \in A_{\text{pi}}, t \in [0, \mathcal{T}].$$

2.2. Valves and Control Valves. Valves $a = (u, v) \in A_{\text{v1}}$ are the most simple controllable elements in the considered gas transport networks. They can be in two different states: open or closed. To describe the behavior in both states, we need the variables $p_{a,u}(t)$ and $p_{a,v}(t)$ modeling the pressure at the in- and outlet of the valve, respectively, as well as the variable $q_a(t)$ modeling the mass flow through the valve. With this notation at hand, we have

$$\begin{aligned}p_{a,u}(t) &= p_{a,v}(t), & \text{if valve } a \text{ is open,} \\ q_a(t) &= 0, & \text{if valve } a \text{ is closed}\end{aligned}$$

for all $t \in [0, \mathcal{T}]$. More detailed information about valves and a formulation as a mixed-integer linear model can be found in [15].

Slightly more complicated than valves are control valves $a = (u, v) \in A_{\text{cv}}$. Their open state is further distinguished into the active state and the bypass mode. If the control valve is active at time $t \in [0, \mathcal{T}]$, it can decrease the incoming gas pressure by a controllable amount $\Delta_a(t) \in [\Delta_a^-, \Delta_a^-]$. Otherwise, i.e., in bypass mode, the control valve acts like an open valve. In summary, we have

$$\begin{aligned}p_{a,u}(t) - \Delta_a(t) &= p_{a,v}(t), & \text{if control valve } a \text{ is active,} \\ p_{a,u}(t) &= p_{a,v}(t), & \text{if control valve } a \text{ is in bypass mode,} \\ q_a(t) &= 0, & \text{if control valve } a \text{ is closed}\end{aligned}$$

for all $t \in [0, \mathcal{T}]$. More detailed information about control valves and a specific mixed-integer linear model formulation can again be found in [15].

2.3. Compressor Machines. Compressor machines $a = (u, v) \in A_{\text{cm}}$ are used to increase the inflow gas pressure to a higher outflow pressure. As control valves, a compressor machine can be active, closed, or in bypass mode. If the compressor machine is in active status, it can increase the gas pressure by $\Delta_a(t)$ at time $t \in [0, \mathcal{T}]$. The other states are the same as for control valves:

$$\begin{aligned}p_{a,u}(t) + \Delta_a(t) &= p_{a,v}(t), & \text{if compressor machine } a \text{ is active,} \\ p_{a,u}(t) &= p_{a,v}(t), & \text{if compressor machine } a \text{ is in bypass mode,} \\ q_a(t) &= 0, & \text{if compressor machine } a \text{ is closed.}\end{aligned}$$

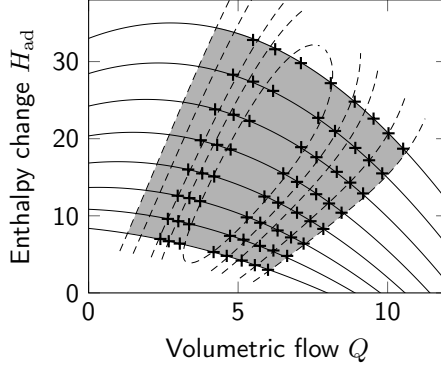


FIGURE 1. Characteristic diagrams of a turbo compressor. The feasible operating range is marked gray.

The modeling of the feasible range of $\Delta_a(t)$ is more complicated. We only consider turbo compressors, which are typically described by so-called characteristic diagrams as shown in Fig. 1. The volumetric flow rate through the unit (x -axis in Fig. 1) is given by

$$Q = \frac{c^2 q_a(t)}{p_{a,u}(t)},$$

where $p_{a,u}(t)$ denotes the inflow pressure of the machine. Moreover, the specific change in adiabatic enthalpy (y -axis in Fig. 1) is modeled by

$$H_{\text{ad}} = R_s T z_m \frac{\kappa}{\kappa - 1} \left[\left(\frac{p_{a,v}(t)}{p_{a,u}(t)} \right)^{\frac{\kappa-1}{\kappa}} - 1 \right],$$

where we assume that the isentropic exponent $\kappa = 1.38$ is constant and where $p_{a,u}(t)$, $p_{a,v}(t)$ denote the inflow and outflow pressure of the compressor unit.

In contrast to control valves, the realizable pressure change in compressors is not modeled independently of the specific flow through the unit; see the gray area in Fig. 1 that depicts the feasible operating range of an exemplary machine. Thus, we have to model the nonlinear boundaries of this region, which we do by using the nonlinear constraints

$$f^i(Q, H_{\text{ad}}) \leq 0, \quad i = 1, \dots, 4.$$

Despite the discussed nonlinearity, tight linear relaxations via outer approximations have been developed in the recent years. We use the formulations developed in [15].

In order to complete the description of all arc models, we finally note that the mass flow on all active arcs are bounded below and above by

$$q_a(t) \in [q_a^-, q_a^+] \quad \text{for all } a \in A_{\text{vl}} \cup A_{\text{cv}} \cup A_{\text{cm}}, \quad t \in [0, \mathcal{T}].$$

2.4. Nodes. At nodes we have to state some continuity conditions. To this end, we introduce node pressure variables

$$p_u(t) \in [p_u^-, p_u^+] \quad \text{for all } u \in V, \quad t \in [0, \mathcal{T}].$$

Continuity of gas pressure along nodes is then given by

$$p_u(t) = p_{a,u}(t) \quad \text{for all } a \in \delta^{\text{in}}(u) \cup \delta^{\text{out}}(u)$$

for all $t \in [0, \mathcal{T}]$. Finally, continuity of mass flows at a node u is described by

$$\begin{aligned} & q_u(t) + \sum_{a \in A_{\text{pi}} \cap \delta^{\text{in}}(u)} q_{a,u}(L_a, t) + \sum_{a \in A_{\text{act}} \cap \delta^{\text{in}}(u)} q_a(t) \\ = & \sum_{a \in A_{\text{pi}} \cap \delta^{\text{out}}(u)} q_a(0, t) + \sum_{a \in A_{\text{act}} \cap \delta^{\text{out}}(u)} q_a(t) \end{aligned}$$

for all $t \in [0, \mathcal{T}]$, where

$$q_u(t) \begin{cases} \geq 0 & \text{for all } u \in V_+, \\ \leq 0 & \text{for all } u \in V_-, \\ = 0 & \text{for all } u \in V_0 \end{cases}$$

is the amount of supplied or discharged or gas at node u and $A_{\text{act}} := A_{\text{cv}} \cup A_{\text{vl}} \cup A_{\text{cm}}$ is used to abbreviate the set of active network elements.

2.5. Objective Functions. There are many reasonable objective functions in gas transport optimization. We are interested in the question whether, given an initial state, the network can be controlled such that another prescribed state can be reached in a certain amount of time. This question is motivated by the desire to satisfy a given demand and related to problems of exact nodal controllability, see, e.g., [21]. Since the aim is to track the desired state, this leads us to tracking-type objective functions. For this, let

$$\hat{p}_{V_{\pm}} := (\hat{p}_u)_{u \in V_{\pm}}, \quad \hat{q}_{V_{\pm}} := (\hat{q}_u)_{u \in V_{\pm}}, \quad V_{\pm} := V_+ \cup V_-$$

describe the state to be reached given as vectors of pressures and mass flows at boundary nodes. Using the analogous notation

$$p_{V_{\pm}}(\mathcal{T}) := (p_u(\mathcal{T}))_{u \in V_{\pm}}, \quad q_{V_{\pm}}(\mathcal{T}) := (q_u(\mathcal{T}))_{u \in V_{\pm}},$$

the tracking-type objective function reads

$$J(p_{V_{\pm}}(\mathcal{T}), q_{V_{\pm}}(\mathcal{T})) := \eta \|p_{V_{\pm}}(\mathcal{T}) - \hat{p}_{V_{\pm}}\| + \mu \|q_{V_{\pm}}(\mathcal{T}) - \hat{q}_{V_{\pm}}\|, \quad (5)$$

where $\eta, \mu \geq 0$ are scaling factors.

For the moment, we do not specify the vector norm. Later, when we want to solve mixed-integer linear problems, compatible norms are the 1- and ∞ -norm.

3. INSTANTANEOUS CONTROL

The problem described in the last section combines discrete decisions and is constrained by a system of time-dependent hyperbolic partial differential equations on a graph. To the best of our knowledge, no general-purpose solution strategies exist to directly tackle such mixed-integer optimal control problems (MIOCPs) on graphs. See, e.g., the recent survey [24] for more details about this and related problem classes.

One remedy is to semi-discretize the problem, i.e., to discretize the time horizon $[0, \mathcal{T}]$. To this end, we consider the set $\mathcal{K} := \{0, \dots, K-1\}$ and the corresponding discretization $0 = t_0, t_1, \dots, t_K = \mathcal{T}$ with $\Delta t_{\kappa} = t_{\kappa+1} - t_{\kappa}$ for all $\kappa \in \mathcal{K}$. The resulting problem is still an MIOCP that is “only” constrained by a system of ordinary differential equations (ODEs) on a graph. Depending on the applied time discretization, this ODE constrained MIOCP is still out of reach for general-purpose methods: even for this discrete-time optimization problem, no published algorithm for its solution seems to be available. The situation changes if we consider optimization problems that arise if we consider the discretized time steps separately. To this aim we now consider an instantaneous control approach, which is stated in an abstract manner in Alg. 1.

Algorithm 1 Instantaneous Control Algorithm

-
- Input:** The original MIOCP, a discretized time horizon, and a semi-discretization scheme for the Euler equations. Initial conditions p_u^0 for all $u \in V$, $q_{a,u}^0, q_{a,v}^0$ for all $a = (u, v) \in A_{\text{pi}}$, and q_a^0 for all $a \in A \setminus A_{\text{pi}}$.
- 1: **for** $\kappa = 0, \dots, K - 1$ **do**
 - 2: Setup the optimization problem $(P^{\kappa+1})$ for time step $t_{\kappa+1}$ that only depends on the state at the previous time step t_κ and solve $(P^{\kappa+1})$.
 - 3: **end for**
-

There are some open questions regarding Alg. 1. First of all: How does the problem $(P^{\kappa+1})$ exactly look like that we have to solve in every iteration of our instantaneous control approach. As we have seen in the previous section, all network elements except for pipes only depend on a single point in time. Moreover, these models can be formulated using mixed-integer linear constraints that do not contain any differential equations. In what follows, we denote this mixed-integer linear constraint set (for time step κ) as

$$A^{\kappa+1} \mathbf{x}^{\kappa+1} + B^{\kappa+1} \mathbf{z}^{\kappa+1} = 0, \quad C^{\kappa+1} \mathbf{x}^{\kappa+1} + D^{\kappa+1} \mathbf{z}^{\kappa+1} \geq 0,$$

where $\mathbf{x}^{\kappa+1}$ and $\mathbf{z}^{\kappa+1}$ are the continuous and discrete variables, respectively. Thus, when considering the objective function (5) we obtain the model

$$\min J^{\kappa+1} \quad \text{s.t.} \quad A^{\kappa+1} \mathbf{x}^{\kappa+1} + B^{\kappa+1} \mathbf{z}^{\kappa+1} = 0, \quad (6a)$$

$$C^{\kappa+1} \mathbf{x}^{\kappa+1} + D^{\kappa+1} \mathbf{z}^{\kappa+1} \geq 0, \quad (6b)$$

$$\mathbf{x}^{\kappa+1} \in \mathbb{R}^{n_x}, \quad \mathbf{z}^{\kappa+1} \in \{0, 1\}^{n_z}, \quad (6c)$$

$$\mathbf{x}^{\kappa+1} \in \mathcal{X}^{\kappa+1}, \quad (6d)$$

where the abstract constraint (6d) models feasibility w.r.t. a suitable chosen semi-discretization of the Euler equations on pipes. Possible concretizations for this abstract constraint set are discussed in the next section. Finally, we have to decide on an objective function for every time step:

$$J^{\kappa+1} := \eta \left\| (p_u(t_{\kappa+1}))_{u \in V_\pm} - (\hat{p}_u)_{u \in V_\pm} \right\| + \mu \left\| (q_u(t_{\kappa+1}))_{u \in V_\pm} - (\hat{q}_u)_{u \in V_\pm} \right\|,$$

where $\eta, \mu > 0$ are penalty parameters.

In order to finally specify Problem (6) we have to specify the abstract constraint $\mathbf{x}^{\kappa+1} \in \mathcal{X}^{\kappa+1}$, i.e., we have to discuss the specific time discretization used to semi-discretize the Euler system (4). Obviously, there is a large number of possible discretizations. In the following section, we concentrate on those that yield tractable models that are to be solved within our instantaneous control approach.

4. DISCRETIZATION

In this section we discuss time discretization schemes that yield tractable problems that are to be solved in the instantaneous control algorithm. After time discretization, we are still faced with a mixed-integer ODE constrained optimization problem; see Model (6). We first characterize solutions of the semi-discretized ODE system that we obtain after applying an implicit Euler discretization in time (see Section 4.1). This characterization is then used to specify modified mixed implicit-explicit Euler discretization in time that yield linear constraints for every pipe within our instantaneous control approach (see Sections 4.2 and 4.3).

The discussed time discretization schemes are non-standard combinations of explicit and implicit Euler discretizations. For the ease of presentation, we drop the arc index a throughout this section.

4.1. Fully Implicit Euler Discretization. We consider System (4), substitute $q \leftarrow q/A$, and abbreviate $\theta = \lambda/D$. System (4) is then equivalent to

$$\begin{aligned}\partial_t p + c^2 \partial_x q &= 0, \\ \partial_t q + \partial_x p &= -\frac{\theta c^2}{2} \frac{q|q|}{p} - \frac{gh'}{c^2} p.\end{aligned}$$

Using time steps Δt_κ , $\kappa \in \mathcal{K}$, an implicit Euler discretization in time yields

$$\begin{aligned}\frac{p_{\kappa+1} - p_\kappa}{\Delta t_\kappa} + c^2 \partial_x q_{\kappa+1} &= 0, \\ \frac{q_{\kappa+1} - q_\kappa}{\Delta t_\kappa} + \partial_x p_{\kappa+1} &= -\frac{\theta c^2}{2} \frac{q_{\kappa+1}|q_{\kappa+1}|}{p_{\kappa+1}} - \frac{gh'}{c^2} p_{\kappa+1},\end{aligned}\tag{7}$$

or, in vector notation,

$$\partial_x \begin{pmatrix} q_{\kappa+1} \\ p_{\kappa+1} \end{pmatrix} + \begin{bmatrix} 0 & \frac{1}{c^2 \Delta t_\kappa} \\ \frac{1}{\Delta t_\kappa} & 0 \end{bmatrix} \begin{pmatrix} q_{\kappa+1} \\ p_{\kappa+1} \end{pmatrix} = \begin{pmatrix} -\frac{\theta c^2}{2} \frac{q_{\kappa+1}|q_{\kappa+1}|}{p_{\kappa+1}} - \frac{gh'}{c^2} p_{\kappa+1} + \frac{q_\kappa}{\Delta t_\kappa} \\ \frac{p_\kappa}{\Delta t_\kappa} \end{pmatrix},\tag{8}$$

under the initial conditions

$$\begin{pmatrix} q_{\kappa+1}(0) \\ p_{\kappa+1}(0) \end{pmatrix} = y_0 \in \mathbb{R} \times \mathbb{R}_{>0}.\tag{9}$$

Theorem 4.1. *Let*

$$\xi(x) = \frac{1}{2} \exp\left(\frac{x}{c \Delta t_\kappa}\right)$$

and

$$\begin{aligned}f(x) &= \frac{p_\kappa(x)}{c^2 \Delta t_\kappa}, \\ g(x, q_{\kappa+1}, p_{\kappa+1}) &= -\frac{\theta c^2}{2} \frac{q_{\kappa+1}(x)|q_{\kappa+1}(x)|}{p_{\kappa+1}(x)} - \frac{gh'}{c^2} p_{\kappa+1}(x) + \frac{q_\kappa(x)}{\Delta t_\kappa}.\end{aligned}$$

Then, the solution of the ODE system (7) under the initial conditions (9) satisfies

$$\begin{aligned}q_{\kappa+1}(x) &= (\xi(x) + \xi(-x)) q_{\kappa+1}(0) + \left(-\frac{1}{c} \xi(x) + \frac{1}{c} \xi(-x)\right) p_{\kappa+1}(0) \\ &\quad + I_q(x, q_{\kappa+1}(x), p_{\kappa+1}(x))\end{aligned}\tag{10}$$

and

$$\begin{aligned}p_{\kappa+1}(x) &= (-c\xi(x) + c\xi(-x)) q_{\kappa+1}(0) + (\xi(x) + \xi(-x)) p_{\kappa+1}(0) \\ &\quad + I_p(x, q_{\kappa+1}(x), p_{\kappa+1}(x))\end{aligned}\tag{11}$$

with

$$\begin{aligned}I_q(x, q_{\kappa+1}(x), p_{\kappa+1}(x)) &= I_q^f(x) + I_q^g(x, q_{\kappa+1}(x), p_{\kappa+1}(x)), \\ I_p(x, q_{\kappa+1}(x), p_{\kappa+1}(x)) &= I_p^f(x) + I_p^g(x, q_{\kappa+1}(x), p_{\kappa+1}(x))\end{aligned}$$

and

$$\begin{aligned}I_q^f(x) &= \int_0^x (\xi(x-s) + \xi(-(x-s))) f(s) ds, \\ I_q^g(x, q_{\kappa+1}(x), p_{\kappa+1}(x)) &= \int_0^x \left(-\frac{1}{c} \xi(x-s) + \frac{1}{c} \xi(-(x-s))\right) g(s, q_{\kappa+1}, p_{\kappa+1}) ds, \\ I_p^f(x) &= \int_0^x (-c\xi(x-s) + c\xi(-(x-s))) f(s) ds, \\ I_p^g(x, q_{\kappa+1}(x), p_{\kappa+1}(x)) &= \int_0^x (\xi(x-s) + \xi(-(x-s))) g(s, q_{\kappa+1}, p_{\kappa+1}) ds.\end{aligned}$$

Proof. Using the abbreviations

$$y := \begin{pmatrix} q_{\kappa+1} \\ p_{\kappa+1} \end{pmatrix}, \quad B := \begin{bmatrix} 0 & \frac{1}{c^2 \Delta t_\kappa} \\ \frac{1}{\Delta t_\kappa} & 0 \end{bmatrix},$$

we see that System (8) is equivalent to

$$\partial_x y + B y = \begin{pmatrix} f \\ g \end{pmatrix}. \quad (12)$$

By Duhamel's formula (see, e.g., [7, Theorem 3.4]) a solution of (12) is given by

$$y(x) = \exp(-Bx) y_0 + \int_0^x \exp(-B(x-s)) \begin{pmatrix} f(s) \\ g(s, q_{\kappa+1}, p_{\kappa+1}) \end{pmatrix} ds, \quad (13)$$

where $y_0 = (q_{\kappa+1}(0), p_{\kappa+1}(0))^\top$ consists of the mass flow and pressure values at the beginning the pipe ($x = 0$). Diagonalization of $-B$ yields

$$-B = SDS^{-1},$$

with

$$S = \begin{bmatrix} -\frac{1}{c} & \frac{1}{c} \\ 1 & 1 \end{bmatrix}, \quad D = \begin{bmatrix} \frac{1}{c\Delta t_\kappa} & 0 \\ 0 & -\frac{1}{c\Delta t_\kappa} \end{bmatrix}, \quad S^{-1} = \begin{bmatrix} -\frac{c}{2} & \frac{1}{2} \\ \frac{c}{2} & \frac{1}{2} \end{bmatrix}$$

and we thus have

$$\begin{aligned} \exp(-Bx) &= \begin{bmatrix} -\frac{1}{c} & \frac{1}{c} \\ 1 & 1 \end{bmatrix} \begin{bmatrix} \exp(\frac{x}{c\Delta t_\kappa}) & 0 \\ 0 & \exp(-\frac{x}{c\Delta t_\kappa}) \end{bmatrix} \begin{bmatrix} -\frac{c}{2} & \frac{1}{2} \\ \frac{c}{2} & \frac{1}{2} \end{bmatrix} \\ &= \begin{bmatrix} \xi(x) + \xi(-x) & -\frac{1}{c}\xi(x) + \frac{1}{c}\xi(-x) \\ -c\xi(x) + c\xi(-x) & \xi(x) + \xi(-x) \end{bmatrix}. \end{aligned}$$

Analogously, we get

$$\exp(-B(x-s)) = \begin{bmatrix} \xi(x-s) + \xi(-(x-s)) & -\frac{1}{c}\xi(x-s) + \frac{1}{c}\xi(-(x-s)) \\ -c\xi(x-s) + c\xi(-(x-s)) & \xi(x-s) + \xi(-(x-s)) \end{bmatrix}.$$

Substituting both matrix exponentials into (13) finally yields the theorem. \square

Implicit Euler discretization in time as considered in the last theorem is a standard approach for the Euler equations in gas transport; see, e.g., [47]. However, for this setting the last theorem does not explicitly state an algebraic solution of the ODE system (8) but gives us some guidance on how to obtain such a formulation. Neglecting the integrals in (10) and (11) would directly yield a linear set of constraints that couple the mass flow and gas pressure values at the end of the pipe ($x = L$) with the values at its beginning ($x = 0$). The nonlinearity (w.r.t. terms of the time step $t_{\kappa+1}$) only appears due to the inhomogeneity g that contains nonlinearities in mass flow $q_{\kappa+1}$ and pressure $p_{\kappa+1}$. Thus, a fix-point equation still has to be solved. This nonlinearity remains independent of whether we use an analytical formula for the antiderivatives of the integrals or whether we use numerical integration schemes like the trapezoidal rule that would still require the evaluation of nonlinearities in $q_{\kappa+1}$ and $p_{\kappa+1}$.

4.2. Mixed Implicit-Explicit Euler Discretization. Guided by the results of the last section we now reduce the resulting nonlinearity in the right-hand side of the semi-discretized system. To this end, we consider the case in which we replace the inhomogeneity $g(x, q_{\kappa+1}, p_{\kappa+1})$ in Theorem 4.1 with $\tilde{g}(x)$ given as

$$\tilde{g}(x) := -\frac{\theta c^2 q_\kappa(x) |q_\kappa(x)|}{2 p_\kappa(x)} - \frac{gh'}{c^2} p_\kappa(x) + \frac{q_\kappa(x)}{\Delta t_\kappa},$$

i.e., we apply an explicit Euler discretization to the right-hand side of the momentum equation in (4):

$$\begin{aligned} \frac{p_{\kappa+1} - p_{\kappa}}{\Delta t_{\kappa}} + c^2 \partial_x q_{\kappa+1} &= 0, \\ \frac{q_{\kappa+1} - q_{\kappa}}{\Delta t_{\kappa}} + \partial_x p_{\kappa+1} &= -\frac{\theta c^2}{2} \frac{q_{\kappa} |q_{\kappa}|}{p_{\kappa}} - \frac{gh'}{c^2} p_{\kappa}. \end{aligned} \quad (14)$$

Applying the same arguments as before we obtain the following result.

Corollary 4.2. *Let ξ , f , and I_q^f as well as $I_p^f(x)$ be given as in Theorem 4.1. Then, the solution of the ODE system (14)*

$$\partial_x \begin{pmatrix} q_{\kappa+1} \\ p_{\kappa+1} \end{pmatrix} + \begin{bmatrix} 0 & \frac{1}{c^2 \Delta t_{\kappa}} \\ \frac{1}{\Delta t_{\kappa}} & 0 \end{bmatrix} \begin{pmatrix} q_{\kappa+1} \\ p_{\kappa+1} \end{pmatrix} = \begin{pmatrix} -\frac{\theta c^2}{2} \frac{q_{\kappa} |q_{\kappa}|}{p_{\kappa}} - \frac{gh'}{c^2} p_{\kappa} + \frac{q_{\kappa}}{\Delta t_{\kappa}} \\ \frac{p_{\kappa}}{c^2 \Delta t_{\kappa}} \end{pmatrix}$$

under the initial conditions

$$\begin{pmatrix} q_{\kappa+1}(0) \\ p_{\kappa+1}(0) \end{pmatrix} = y_0 \in \mathbb{R} \times \mathbb{R}_{>0}$$

is given by

$$q_{\kappa+1}(x) = (\xi(x) + \xi(-x)) q_{\kappa+1}(0) + \left(-\frac{1}{c} \xi(x) + \frac{1}{c} \xi(-x) \right) p_{\kappa+1}(0) + \tilde{I}_q(x)$$

and

$$p_{\kappa+1}(x) = (-c\xi(x) + c\xi(-x)) q_{\kappa+1}(0) + (\xi(x) + \xi(-x)) p_{\kappa+1}(0) + \tilde{I}_p(x)$$

with

$$\tilde{I}_q(x) = I_q^f(x) + \tilde{I}_q^g(x), \quad \tilde{I}_p(x) = I_p^f(x) + \tilde{I}_p^g(x)$$

and

$$\begin{aligned} \tilde{I}_q^g(x) &= \int_0^x \left(-\frac{1}{c} \xi(x-s) + \frac{1}{c} \xi(-(x-s)) \right) \tilde{g}(s) ds, \\ \tilde{I}_p^g(x) &= \int_0^x (\xi(x-s) + \xi(-(x-s))) \tilde{g}(s) ds. \end{aligned}$$

The latter theorem reveals the fact that an explicit discretization of the source terms yield solutions $q_{\kappa+1}(x)$ and $p_{\kappa+1}(x)$ that depend linearly on the (spatial) initial values $q_{\kappa+1}(0)$ and $p_{\kappa+1}(0)$ because the integrals only depend on the solution of the previous time step, i.e., on q_{κ} and p_{κ} . These two quantities are known at the beginning and at the end of the pipe as a result of the problem solved in the last step of the instantaneous control approach. Thus, the integrals $\tilde{I}_q(L_a)$ and $\tilde{I}_p(L_a)$ can be evaluated using the trapezoidal rule, yielding $\hat{I}_q(L_a)$ and $\hat{I}_p(L_a)$. We see that we obtained the affine-linear set of constraints

$$\begin{aligned} q_{a,v}(t_{\kappa+1}) &= (\xi(L_a) + \xi(-L_a)) q_{a,u}(t_{\kappa+1}) \\ &\quad + \left(-\frac{1}{c} \xi(L_a) + \frac{1}{c} \xi(-L_a) \right) p_{a,u}(t_{\kappa+1}) \\ &\quad + \hat{I}_q(L_a), \end{aligned} \quad (15)$$

and

$$\begin{aligned} p_{a,v}(t_{\kappa+1}) &= (-c\xi(L_a) + c\xi(-L_a)) q_{a,u}(t_{\kappa+1}) \\ &\quad + (\xi(L_a) + \xi(-L_a)) p_{a,u}(t_{\kappa+1}) \\ &\quad + \hat{I}_p(L_a) \end{aligned} \quad (16)$$

for every pipe $a = (u, v) \in A_{\text{pi}}$. Hence, we have found an affine-linear representation of gas dynamics in the variables

$$q_{a,u}(t_{\kappa+1}), \quad p_{a,u}(t_{\kappa+1}), \quad q_{a,v}(t_{\kappa+1}), \quad p_{a,v}(t_{\kappa+1}).$$

4.2.1. *Steady-State Consistent Ansatz Functions for Numerical Integration.* The usage of the trapezoidal rule to evaluate the integrals in (15) and (16) is motivated by the fact that the only values of the functions $q_\kappa(x)$ and $p_\kappa(x)$ (with $x \in [0, L]$) we know are those for $x \in \{0, L\}$. The trapezoidal rule corresponds to a linear interpolation of the points $(0, p_\kappa(0))$ and $(L, p_\kappa(L))$ (and analogously for q_κ).

Another ansatz function that one may use is motivated by steady-state solutions of the Euler equations; see, e.g. [12, 45]. Using suitable assumptions, it is known that the stationary variant

$$\begin{aligned}\partial_x q &= 0, \\ \partial_x p &= -\frac{\theta c^2}{2} \frac{q|q|}{p} - \frac{gh'}{c^2} p\end{aligned}$$

of System (4) with initial values $q(0)$ and $p(0)$ has the solution

$$q(x) = \text{const}$$

and

$$p(x) = \sqrt{p(0)^2 - c^2 \theta q(x)|q(x)|} x \quad (17)$$

for $h' = 0$ as well as

$$p(x) = \sqrt{p(0)^2 - c^2 \theta q(x)|q(x)|} (\exp(\tilde{S}x) - 1) / \tilde{S} \sqrt{\exp(-\tilde{S}x)}, \quad (18)$$

for $h' \neq 0$, where the abbreviation $\tilde{S} = (2gh')/c^2$ is used. These formulas for the pressure drop are known as the Weymouth equations.

It is also possible to use these functions as steady-state consistent ansatz functions for numerical integration. This means that the points used for numerical integration satisfy the steady-state equations, which can be achieved as follows. If the flow \tilde{q}_κ is constant in x (which also implies $q_\kappa(0) = q_\kappa(L)$), the pressure values used for numerical integration should satisfy the stationary pressure drop relation given in (17) or (18), respectively. Thus, by using the linear interpolation

$$\tilde{q}_\kappa(x) = q_\kappa(0) + \frac{x}{L}(q_\kappa(L) - q_\kappa(0))$$

for the flows (as it is the case for the trapezoidal rule) and then applying this flow approximation to the pressure formula (17) or (18), i.e.,

$$\tilde{p}_\kappa(x) = \sqrt{p_\kappa(0)^2 - c^2 \theta \tilde{q}_\kappa(x)|\tilde{q}_\kappa(x)|} x$$

for $h' = 0$ as well as

$$\tilde{p}_\kappa(x) = \sqrt{p_\kappa(0)^2 - c^2 \theta \tilde{q}_\kappa(x)|\tilde{q}_\kappa(x)|} (\exp(\tilde{S}x) - 1) / \tilde{S} \sqrt{\exp(-\tilde{S}x)}$$

for $h' \neq 0$ yields values $q_\kappa(0), \tilde{q}_\kappa(L), p_\kappa(0)$, and $\tilde{p}_\kappa(L)$ (or even more values $\tilde{q}_\kappa(x), \tilde{p}_\kappa(x)$ for $x \in (0, L)$) that are consistent with the steady states in (17) or (18) and that can be used for our numerical integration.

4.3. Mixed Implicit-Explicit Euler Discretization of the Source Terms.

Regarding the two last time discretization schemes, i.e., the fully implicit and the mixed implicit-explicit scheme, one may also think of a further intermediate case. We now show that this intermediate case also yields affine-linear formulations of the pipe's outflow values in dependence of the corresponding inflow values.

To this end, we apply a mixed explicit-implicit discretization of the source term of the momentum equation and obtain the ODE system

$$\frac{p_{\kappa+1} - p_\kappa}{\Delta t_\kappa} + c^2 \partial_x q_{\kappa+1} = 0, \quad (19)$$

$$\frac{q_{\kappa+1} - q_\kappa}{\Delta t_\kappa} + \partial_x p_{\kappa+1} = -\frac{\theta c^2}{2} \frac{|q_\kappa| q_{\kappa+1}}{p_\kappa} - \frac{gh'}{c^2} p_\kappa. \quad (20)$$

This can be written in vector form as

$$\partial_x \begin{pmatrix} q_{\kappa+1} \\ p_{\kappa+1} \end{pmatrix} + \begin{bmatrix} 0 & \frac{1}{c^2 \Delta t_\kappa} \\ \frac{1}{\Delta t_\kappa} + \frac{c^2 \theta |q_\kappa|}{2 p_\kappa} & 0 \end{bmatrix} \begin{pmatrix} q_{\kappa+1} \\ p_{\kappa+1} \end{pmatrix} = \begin{pmatrix} -\frac{gh'}{c^2} \frac{p_\kappa}{\Delta t_\kappa} \\ -\frac{gh'}{c^2} p_\kappa + \frac{q_\kappa}{\Delta t_\kappa} \end{pmatrix}. \quad (21)$$

The initial conditions are again given by

$$\begin{pmatrix} q_{\kappa+1}(0) \\ p_{\kappa+1}(0) \end{pmatrix} = y_0 \in \mathbb{R} \times \mathbb{R}_{>0}.$$

The main difference w.r.t. System (8) obtained using the mixed implicit-explicit discretization is the dependence of the system matrix on x due to the appearing functions p_κ and q_κ .

Using the notation

$$M(x) = \begin{bmatrix} 0 & \frac{1}{c^2 \Delta t_\kappa} \\ \frac{1}{\Delta t_\kappa} + \frac{c^2 \theta |q_\kappa(x)|}{2 p_\kappa(x)} & 0 \end{bmatrix}, \quad h(x) = -\frac{gh'}{c^2} p_\kappa(x) + \frac{q_\kappa(x)}{\Delta t_\kappa}$$

and f as well as y as before, System (21) reads

$$\partial_x y(x) + M(x)y(x) = \begin{pmatrix} f(x) \\ h(x) \end{pmatrix}.$$

Denote $F(x) := \int_0^x -M(s) ds$. Then a solution is given by

$$y(x) = \exp(F(x)) \left(y_0 + \int_0^x \exp(-F(s)) \begin{pmatrix} f(s) \\ h(s) \end{pmatrix} ds \right).$$

Given this solution, the question is how to obtain an affine-linear constraint set as in Section 4.2. The idea is again to use numerical integration. First, we approximate $F(L)$ and the inner integral using the trapezoidal rule, i.e.,

$$\exp(F(L)) \approx \exp\left(-\frac{L}{2}(M(0) + M(L))\right)$$

and

$$\int_0^L \exp(-F(s)) \begin{pmatrix} f(s) \\ h(s) \end{pmatrix} ds \approx \frac{L}{2} \left(\exp(-F(L)) \begin{pmatrix} f(L) \\ h(L) \end{pmatrix} + \exp(-F(0)) \begin{pmatrix} f(0) \\ h(0) \end{pmatrix} \right).$$

After applying these numerical integrations (together with the computation of the matrix exponentials) we finally obtain the affine-linear formulation

$$\begin{aligned} y(L) &= \begin{pmatrix} q_{\kappa+1}(L) \\ p_{\kappa+1}(L) \end{pmatrix} \approx \exp\left(-\frac{L}{2}(M(0) + M(L))\right) \begin{pmatrix} q_{\kappa+1}(0) \\ p_{\kappa+1}(0) \end{pmatrix} \\ &+ \frac{L}{2} \exp\left(-\frac{L}{2}(M(0) + M(L))\right) \left(\exp(-F(L)) \begin{pmatrix} f(L) \\ h(L) \end{pmatrix} + \exp(-F(0)) \begin{pmatrix} f(0) \\ h(0) \end{pmatrix} \right). \end{aligned}$$

5. EXISTENCE AND UNIQUENESS OF THE SEMI-DISCRETIZED SYSTEM ON NETWORKS

The results in the last section reveal that there exist time discretization schemes that yield affine-linear models of gas physics in pipes in an instantaneous control approach. The keys to this result are Theorem 4.1 and Corollary 4.2 that characterize or explicitly state solutions of the ODE system on a single pipe. By this, solutions of these ODE systems on single pipes exist and are unique.

The question remains whether the corresponding ODE systems in a network that induces further continuity conditions on nodes is well-posed as well. In this section, we prove that this is the case for the linear model that results from the mixed implicit-explicit time discretization in Section 4.2; see Corollary 4.2. The proof is given for passive networks only, i.e., we have $A = A_{\text{pi}}$, but we discuss extensions to the active case afterward. To this aim, we consider System (14). We neglect the

index $\kappa + 1$ as it represents the actual unknown variables. We differentiate the first equation with respect to x and obtain

$$\begin{aligned}\partial_x p + \Delta t_\kappa c^2 \partial_{xx} q &= \partial_x p_\kappa, \\ q + \Delta t_\kappa \partial_x p &= -\Delta t_\kappa \left(\frac{\theta c^2}{2} \frac{q_\kappa |q_\kappa|}{p_\kappa} + \frac{gh'}{c^2} p_\kappa \right) + q_\kappa.\end{aligned}$$

Using the first equation in the second, we arrive at

$$q - \Delta t_\kappa^2 c^2 \partial_{xx} q = -\Delta t_\kappa \left(\frac{\theta c^2}{2} \frac{q_\kappa |q_\kappa|}{p_\kappa} + \frac{gh'}{c^2} p_\kappa \right) + q_\kappa - \Delta t_\kappa \partial_x p_\kappa. \quad (22)$$

Thus, the system can be reduced to a single equation of second order in space. Indeed, (22) is an elliptic (ordinary) differential equation. We now turn to the graph representation. For this, we need to split the node set V into the set of simple nodes $V^S := \{u \in V : |\delta(u)| = 1\}$ and the set of nodes $V^M = V \setminus V^S$ with more than one incident arc. Here and in what follows, we set $\delta(u) := \delta^{\text{in}}(u) \cup \delta^{\text{out}}(u)$.

Without loss of generality, we assume that there is only demand and supply at simple nodes $u \in V^S$. Thus, at nodes $u \in V^M$ we have the transmission conditions

$$p_{a,u} - p_{a',u} = 0 \quad \text{for all } a, a' \in \delta(u), \quad (23)$$

$$\sum_{a \in \delta^{\text{in}}(u)} q_{a,u} - \sum_{a \in \delta^{\text{out}}(u)} q_{a,u} = 0. \quad (24)$$

We may now rewrite the transmission conditions in terms of the mass flows using the continuity equation (19). As the pressures of the last time step satisfy the transmission conditions (23), we have

$$\partial_x q_{a,u} = \partial_x q_{a',u} \quad \text{for all } u \in V^M, \ a, a' \in \delta^{\text{in}}(u) \cup \delta^{\text{out}}(u),$$

in addition to the classical flow conservation condition (24). We are now ready to write down the full system on the graph. Defining

$$f_a := -\Delta t_\kappa \left(\frac{\theta_a c^2}{2} \frac{q_{a,\kappa} |q_{a,\kappa}|}{p_{a,\kappa}} + \frac{gh'_a}{c^2} p_{a,\kappa} \right) + q_{a,\kappa} - \Delta t_\kappa \partial_x p_{a,\kappa}, \quad \gamma := \Delta t_\kappa^2 c^2$$

for $a \in A$ and $x \in (0, 1)$ we then obtain the system

$$q_a - \gamma \partial_{xx} q_a = f_a \quad \text{for all } a \in A, x \in (0, 1), \quad (25a)$$

$$\partial_x q_{a,u} - \partial_x q_{a',u} = 0 \quad \text{for all } u \in V^M, \ a, a' \in \delta(u), \quad (25b)$$

$$\sum_{a \in \delta^{\text{in}}(u)} q_{a,u} - \sum_{a \in \delta^{\text{out}}(u)} q_{a,u} = 0 \quad \text{for all } u \in V^M, \quad (25c)$$

$$q_{a,u} = \omega_u \quad \text{for all } u \in V_D^S, \ a \in \delta(u), \quad (25d)$$

$$\partial_x q_{a,u} = \omega_u \quad \text{for all } u \in V_N^S, \ a \in \delta(u), \quad (25e)$$

Where $\omega_u \in \mathbb{R}$ denotes the Dirichlet data for $u \in V_D^S$ and the Neumann data for $u \in V_N^S$, respectively. For this, the set of simple nodes was split into Dirichlet nodes V_D^S and Neumann nodes V_N^S . The problem of well-posedness for the discretized system (14) on the graph G reduces to the well-posedness of the linear elliptic system (25) on the same graph. System (25) with transmission conditions (25b) replaced with the classical conditions (23) has been analyzed in the literature; see, e.g., [30]. It turns out that, in this case, for any graph G such that each node is connected to a Dirichlet node by a simple path, the underlying elliptic operator is self-adjoint and positive definite. Thus, the problem admits a unique solution. The same argument holds true in case of (25), as the transmission conditions in (25)

also lead to a self-adjoint and positive definite operator on the graph G . Using the notation

$$d_{a,u} = \begin{cases} 1, & \text{if } a = (u, v) \text{ for some } v \in V, \\ -1, & \text{if } a = (v, u) \text{ for some } v \in V, \\ 0, & \text{else,} \end{cases}$$

one can verify that, indeed, the Lagrange identity

$$\begin{aligned} \langle \mathcal{A}q, \phi \rangle &:= \sum_{a \in A} \int_0^{L_a} (q_a - \gamma \partial_{xx} q_a) \phi_a \, dx \\ &= \sum_{u \in V} \sum_{a \in \delta(u)} d_{a,u} \gamma \partial_x q_{a,u} \phi_{a,u} + \sum_{a \in A} \int_0^{L_a} (q_a \phi_a + \gamma \partial_x q_a \partial_x \phi_a) \, dx \\ &= \sum_{u \in V} \sum_{a \in \delta(u)} d_{a,u} \gamma \partial_x q_{a,u} \phi_{a,u} - \sum_{u \in V} \sum_{a \in \delta(u)} d_{a,u} \gamma q_{a,u} \partial_x \phi_{a,u} + \langle q, \mathcal{A}\phi \rangle \\ &= \langle q, \mathcal{A}\phi \rangle \end{aligned}$$

holds for all $q, \phi \in \mathcal{D}(\mathcal{A})$, where the domain $\mathcal{D}(\mathcal{A})$ is given by

$$\begin{aligned} \mathcal{D}(\mathcal{A}) &:= \{q = (q_a)_{a \in A} \in \Pi_{a \in A} H^2(0, L_a) : \\ &\quad q_{a,u} = 0, \quad u \in V_D^S, \quad a \in \delta(u), \\ &\quad \partial_x q_{a,u} = 0, \quad u \in V_N^S, \quad a \in \delta(u), \\ &\quad \partial_x q_{a,u} = \partial_x q_{a',u}, \quad u \in V^M, \quad a, a' \in \delta(u), \\ &\quad \sum_{a \in \delta^{\text{in}}(u)} q_{a,u} = \sum_{a \in \delta^{\text{out}}(u)} q_{a,u}, \quad u \in V^M\} \end{aligned}$$

Thus, we can define the unbounded and self-adjoint operator

$$\mathcal{A}q := (q_a - \gamma \partial_{xx} q_a)_{a \in A}$$

with domain $\mathcal{D}(\mathcal{A})$ in the Hilbert space $\mathcal{H} := \Pi_{a \in A} L^2(0, L_a)$. This operator satisfies $\langle \mathcal{A}q, q \rangle \geq \|q\|_{\mathcal{H}}^2$. Using the energy space

$$\begin{aligned} \mathcal{V} &:= \{q = (q_a)_{a \in A} \in \Pi_{a \in A} H^1(0, L_a) : \\ &\quad q_{a,u} = 0, \quad u \in V_D^S, \quad a \in \delta(u), \\ &\quad \partial_x q_{a,u} = 0, \quad u \in V_N^S, \quad a \in \delta(u), \\ &\quad \sum_{a \in \delta^{\text{in}}(u)} q_{a,u} = \sum_{a \in \delta^{\text{out}}(u)} q_{a,u}, \quad u \in V^M\} \end{aligned}$$

we have shown the following well-posedness result.

Theorem 5.1. *Let a gas network $G = (V, A)$ be given such that each node is connected to a Dirichlet node by a simple path. Moreover, let controls ω_u , $u \in V^S$, and right-hand sides $f \in \mathcal{H}$ be given. Then, there exists a unique solution $q \in \mathcal{D}(\mathcal{A})$ of System (25). If $f \in \mathcal{V}^*$, then there is a unique solution $q \in \mathcal{V}$.*

Before we close this section let us briefly discuss the case of networks that also comprise active elements like valves, control valves, and compressors. All of them can be operated in bypass mode (or be simply open in the case of valves). The bypass case in which no pressure difference appears and in which no further constraints regarding in- and outflows are present coincides with the case of Theorem 5.1 on a slightly modified graph, in which we identify nodes that are connected with such a bypass. If the valves are closed this corresponds to a change of the topology of the network, in which the corresponding arcs are removed. Again, Theorem 5.1 applies. The case with active compressors is more involved and not discussed in this article.

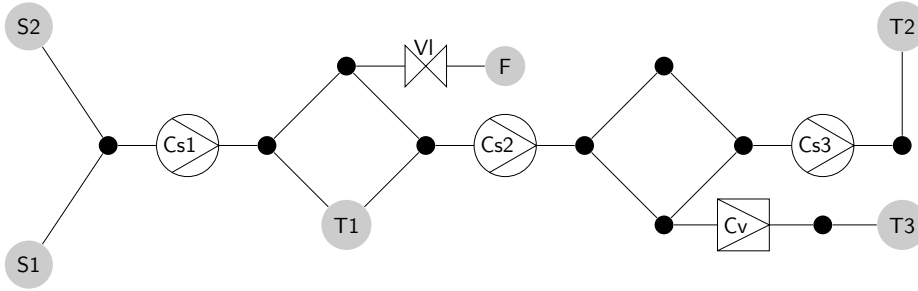


FIGURE 2. Test network: All entry and exit nodes are marked gray and all smaller black nodes are inner nodes. Arcs without technical symbol are pipes.

6. COMPUTATIONAL RESULTS

In this section we consider case studies to illustrate the applicability of our instantaneous control approach to realistic control problems. Throughout this section, we consider the test network given in Figure 2. The network is taken from [10]. It contains 16 nodes: 2 entries (S1, S2), 3 exits (T1, T2, T3), and one flexible boundary (F) that can be entry and exit over time.¹ All remaining nodes (10) are inner nodes. The nodes are connected by 17 arcs that comprise 12 pipes, 3 compressors (Cs1, Cs2, Cs3), one valve (V), and one control valve (Cv). The total pipe length is 92 km with separate pipe varying between 5 km to 12 km. The pipes' diameters vary between 0.5 m to 1.1 m and the roughness values lie between 0.01 mm to 0.05 mm. The planning horizon is 3 hours that we split in three consecutive time intervals of 1 hour with separate control targets. We choose a time discretization of 1 min and a spatial discretization of 100 m yielding 180 time intervals and in total 920 spatial intervals. For the ease of implementation the discussed results all have been obtained with the mixed implicit-explicit time discretization (14) presented in Section 4.2. It is also an interesting question how the results of the chosen discretization compares to the results of other MIP-compatible schemes that are discussed in Section 4. However, a detailed numerical comparison is out of scope of this paper and topic of future research.

The initial state is a stationary state of the network in which all active elements are open and inactive, i.e., the valve is open, and all compressor stations and the control valve are in bypass mode. The entry S1 supplies 96 kg s^{-1} and entry S2 delivers 19 kg s^{-1} . The exit customers T1 and T3 only withdraw small amounts of 2 kg s^{-1} and 4 kg s^{-1} , respectively, whereas exit T2 models a large industrial customer that withdraws 108 kg s^{-1} . Since the flow values in the initial state are comparably small and all compressors are in bypass mode, all pressure values are around 60 bar.

Our instantaneous control approach and all models have been implemented using the C++ framework LaMaTTO++ for modeling and solving mixed-integer nonlinear optimization problems on networks [31]. All MIP models have been solved with Gurobi 6.5.0 [20] using all available threads. All MIPs of the separate time steps are of same size: 2316 variables and 2460 constraints. The constraint matrix has 7735 non-zeros. Gurobi's presolve typically removes approximately 280 variables and 240 constraints. Approximately 5% of all variables are binaries. We remark that a fully coupled time-discretized problem would consist of more than 400 000 constraints,

¹We remark that the consideration of flexible nodes is not completely in line with the network model presented in Section 2 because $u \in V_-$ or $u \in V_+$ for a node $u \notin V_0$ does not hold anymore for all time steps. However, all required changes in the model are straightforward.

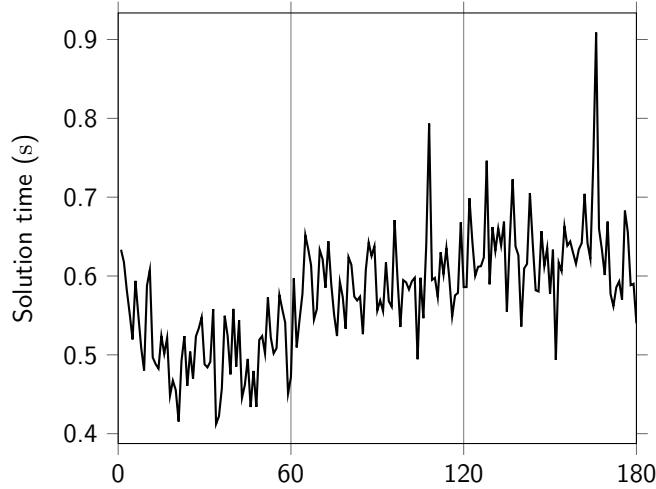


FIGURE 3. Gurobi's running times for solving all time-discrete MIPs (for t_1, \dots, t_{180}) of the instantaneous control method

almost 450 000 variables (out of which approximately 20 000 would be binary), and additional nonlinearities. The comparably small size of the single MIPs yield fast solution times. All computations have been performed on an Intel[®] Core[™] i5-3360M CPU with 4 cores and 2.8 GHz each and 4 GB RAM. The running times of all 180 MIPs are given in Figure 3. All of them lie between 0.4 s to 0.9 s with an aggregated running time of 104 s.

Before we describe the results in detail, we have to discuss some technical issues regarding the chosen objective function. We use the tracking type function of Section 2.5 with $\mu \gg \eta$, i.e., we penalize deviations of the target flows much harder than deviations in target pressure. Moreover, we allow different penalty parameters μ_u and η_u for all nodes $u \in V_{\pm}$ in order to put more emphasis on the control of certain nodes. Finally, we use the max-norm in (5), i.e.,

$$\min_{x, y \in \mathbb{R}^n} \|x - y\|_{\infty}, \quad \|x - y\|_{\infty} := \max_{i=1, \dots, n} |x_i - y_i|$$

that we equivalently reformulate by minimizing the auxiliary variable $w \in \mathbb{R}_{\geq 0}$ and additionally imposing the constraints

$$x_i - y_i = z_i, \quad z_i = z_i^+ - z_i^-, \quad z_i^+, z_i^- \geq 0, \quad z_i^+ + z_i^- \leq w$$

for all $i = 1, \dots, n$ that make use of the auxiliary variables $z_i, z_i^+, z_i^- \in \mathbb{R}$.

We now turn to the discussion of the results of the instantaneous control approach. First, we have to note that the instantaneous control approach will obviously have limitations in reaching terminal states that require an action early in the control period or that considerably differ from the initial state. This is why we split the time horizon of 3 hours into 3 blocks of 1 hour each and state a new tracking target in every control sub-period, i.e., in every hour. On the other hand, in real-time operations this strategy may be used to address uncertainties that realize during the considered overall time horizon.

As already discussed in the description of the initial state we start with an almost equal pressure of approximately 60 bar at all nodes. The pressure and flow profiles of all entries and exits as well as all the pressure difference profiles for the compressor stations and the control valve are given in Figure 4. The first state that we reach is a higher pressure of 65 bar for the exit customer at T1. All other pressures may be adjusted as required within certain technical bounds that ensure the validity of our

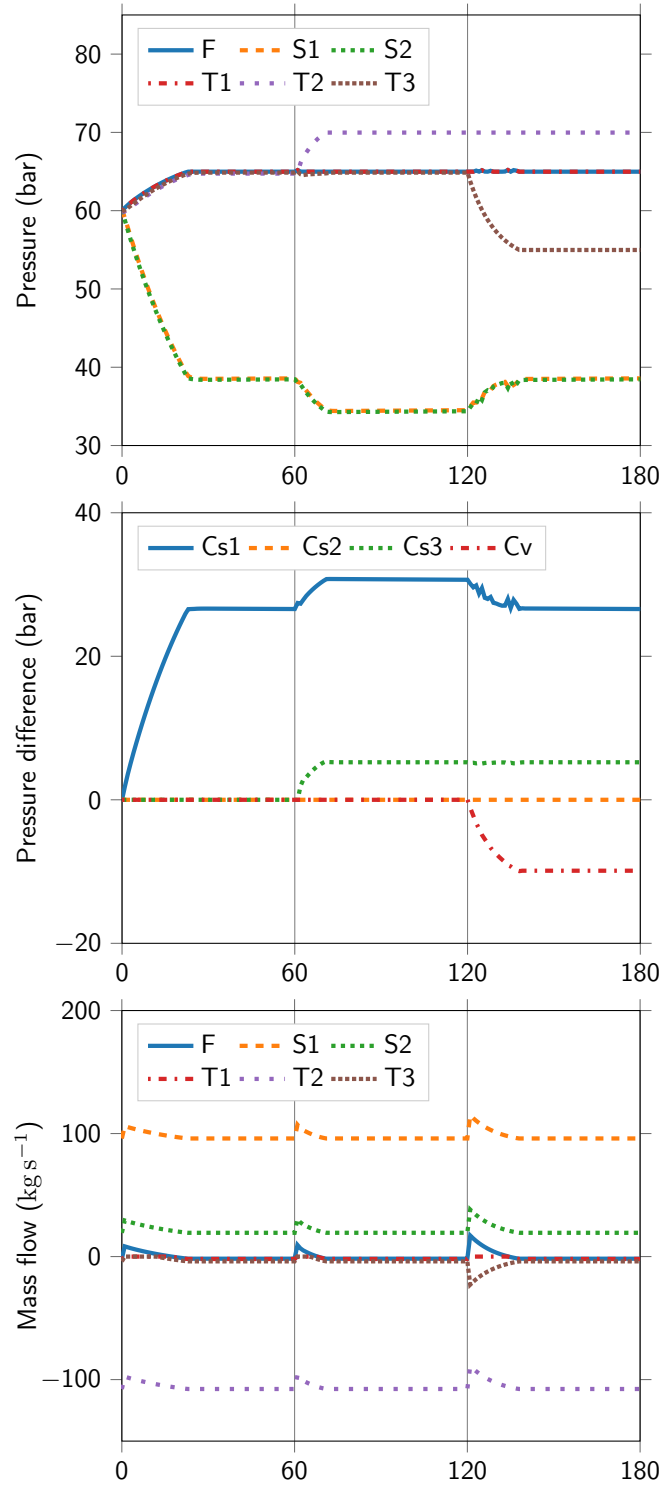


FIGURE 4. Pressures at boundary nodes (top), pressure differences at active elements (middle) and mass flows at boundary node (bottom) over the time horizon (x -axes: 3 h in minutes)

physics model and the penalty parameters μ are chosen such that the amount of supplied and discharged flows stay almost constant over time. In Figure 4 (top) we see that the desired state is achieved after less than half an hour. The main burden lies on the compressor station Cs1 that directly starts compression; see Figure 4 (middle). To this end, it uses the gas in its inflow edges to obtain the required downstream pressure, which yields a pressure drop at the upstream entry nodes as it can be seen in Figure 4 (top). In Figure 4 (bottom) it is also visible that all nodes shortly deliver more or withdraw less gas to increase the overall amount of gas in the network and, thus, the pressure level. Taking a last look at the top figure we also see that all downstream pressures of Cs1 stabilize in a similar way than the outflow pressure at T1 yielding a new stationary state.

The next state to reach is an even higher outflow pressure (70 bar) at exit customer node T2. To achieve this goal similar phenomena as before can be observed. The compressor station Cs3 also starts to compress; see Figure 4 (top and middle). As before, this leads to decreased pressures in the upstream pipes of Cs3, which is the reason why the already running compressor station Cs1 further increases its compression ratio in order to preserve the target pressure at T1 of the previous control period. Activating Cs3 instead of Cs2 follows the intuition that the shortest control period required is achieved if the “nearest” active network device is used. The in- and outflows are also used shortly to fill the pipes with additional gas to boost the pressure level throughout the network before all in- and outflow pressure and mass flow profiles stabilize in a new stationary state.

Starting with this state we finally try to control the network towards a stationary state in which the outflow pressure at the exit node T3 is decreased to 55 bar. The main device used to reach this state is the control valve Cv. It directly starts to decrease its outflow pressure to the required level (Figure 4; top and middle). This also yields increased pressures in the upstream pipes of Cv, which, in turn, lead to the situation that the upstream compressor station Cs1 does not need to preserve its high pressure ratio of the previous control period.

At the beginning of the of third control period we observe some irregular behavior of the compressor station Cs1. This chattering is not a desirable behavior, especially for the active compressors, but currently nothing in our model avoids this behavior, especially because the max-norm objective function typically does not yield unique solutions in a MIP context. However, regularizing objective terms and/or constraints that smooth out these aspects can be easily added to our model if required. A video of the resulting network state over time is available online.²

To conclude our discussion of the ability of our instantaneous control approach, we plot the pressure differences of the respective initial and desired target state over time in Figure 5. It can clearly be seen that, despite the behavior in control period 2 at the very beginning of that period, we always observe a slightly superlinear decrease in the difference to the target state.

As a second case study, we also analyze the observability of the physical phenomenon of pressure and flow waves within a single pipe. To this end, we use a pipe with a length of 10 km, a diameter of 0.7 m, and a roughness of 0.1 mm. Between the first and the fifth second 600 kg s^{-1} are supplied at the pipe’s inlet and 200 kg s^{-1} are supplied in the initial second and from second 6 on. We choose a time discretization of 1 s and spatial discretization of 5 m. Using these high resolutions, our model is able to observe flow and pressure waves within pipes as shown in Figure 6.

To subsume, we see that our instantaneous control method yields plausible physical solutions and allows for controlling between different stationary states that do not differ too much. The comparison of the time required to control a gas network

²http://www.mso.math.fau.de/fileadmin/wima/data_members/schmidt/inst-control.mp4

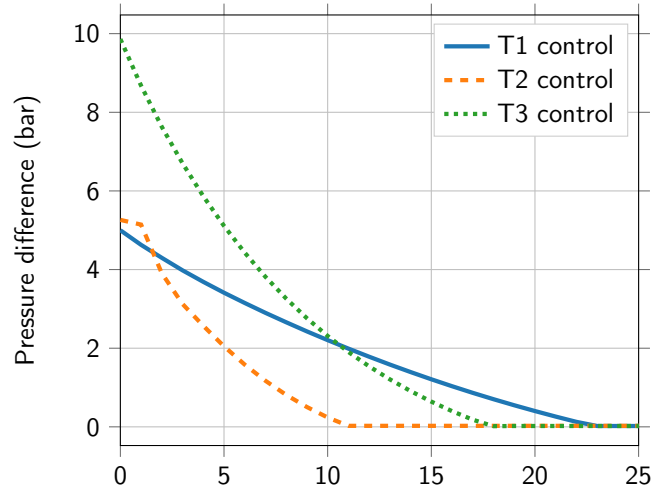


FIGURE 5. Pressure difference (y -axis; in bar) of initial and target state for the three control periods over time (x -axis; in minutes)

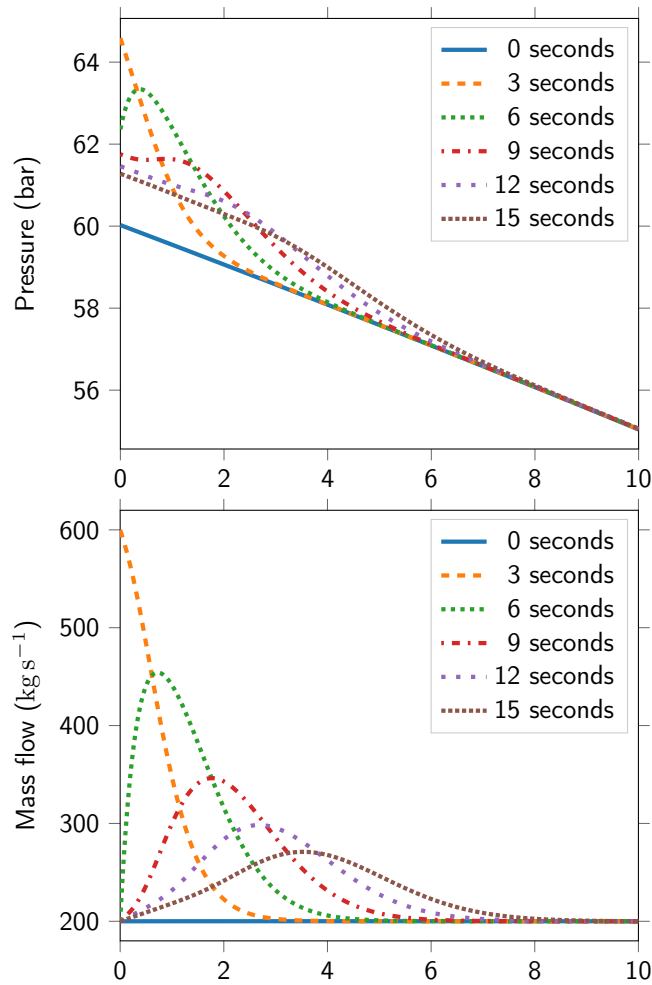


FIGURE 6. Pressure and flow (y -axis) in a single pipe over its length (x -axis in km) for different time points

and the computation times of our method additionally suggests that the approach can indeed be used for online control of realistic gas networks with discrete and continuous controls.

7. CONCLUSION

There is no doubt that mixed-integer optimal control problems that are constrained by systems of partial differential equations on a graph are extremely challenging. The transient control of gas networks that we considered in this paper is a specific instance of the above mentioned problem class. Our contribution is an approach to combine the aspects that make the problem hard: discrete controls with nonlinear physics described by time-dependent differential equations. The proposed instantaneous control method together with suitable time discretizations of the networked PDE systems allows to re-use mixed-integer linear techniques for stationary versions of the problem that have been developed in the last years. We have shown the existence and uniqueness of affine-linear solutions of suitable time-discretized variants of the problem and illustrated that the resulting MIP-based algorithm is capable of effectively controlling realistic gas networks.

A lot of research still remains to be done. We sketch two branches of future work: First, our instantaneous control method is a special case of so-called model predictive or receding horizon control and one drawback of our method is the minimum time window size that we consider in instantaneous control. Thus, the question arises whether there are suitable, i.e., theoretically rigorous and computationally tractable, generalizations of our method to larger time windows. Second, if one adheres to instantaneous control, the obvious question arises on how to effectively solve the mixed-integer nonlinear problems that occur in every time step if we choose standard implicit Euler discretizations in time.

ACKNOWLEDGMENTS

We acknowledge funding through the DFG SFB/Transregio 154, Subprojects A05, B07, B08, and C03. This research has been performed as part of the Energie Campus Nürnberg and supported by funding through the “Aufbruch Bayern (Bavaria on the move)” initiative of the state of Bavaria. Finally, we thank Marc Steinbach for the provision of some data that we used for our numerical studies.

REFERENCES

- [1] N. Altmüller, L. Grüne, and K. Worthmann. “Instantaneous control of the linear wave equation.” In: *Proceedings of MTNS*. 2010.
- [2] M. K. Banda and M. Herty. “Multiscale modeling for gas flow in pipe networks.” In: *Mathematical Methods in the Applied Sciences* 31 (Aug. 2008), pp. 915–936. DOI: 10.1002/ma.948.
- [3] M. K. Banda, M. Herty, and A. Klar. “Gas flow in pipeline networks.” In: *Networks and Heterogeneous Media* 1.1 (Mar. 2006), pp. 41–56. DOI: 10.3934/nhm.2006.1.41.
- [4] B. Baumrucker and L. Biegler. “MPEC strategies for cost optimization of pipeline operations.” In: *Computers & Chemical Engineering* 34.6 (2010), pp. 900–913. DOI: 10.1016/j.compchemeng.2009.07.012.
- [5] J. Brouwer, I. Gasser, and M. Herty. “Gas Pipeline Models Revisited: Model Hierarchies, Nonisothermal Models, And Simulations of Networks.” In: *Multiscale Model. Simul.* 9.2 (2011), pp. 601–623.
- [6] H. Choi, M. Hinze, and K. Kunisch. “Instantaneous control of backward-facing step flows.” In: *Applied Numerical Mathematics* 31.2 (1999), pp. 133–158. DOI: 10.1016/S0168-9274(98)00131-7.

- [7] E. A. Coddington and R. Carlson. *Linear ordinary differential equations*. SIAM, 1997.
- [8] P. Domschke, B. Geißler, O. Kolb, J. Lang, A. Martin, and A. Morsi. “Combination of Nonlinear and Linear Optimization of Transient Gas Networks.” In: *INFORMS Journal on Computing* 23.4 (2011), pp. 605–617. DOI: 10.1287/ijoc.1100.0429.
- [9] K. Ehrhardt and M. C. Steinbach. “KKT Systems in Operative Planning for Gas Distribution Networks.” In: *Proc. Appl. Math. Mech.* 4.1 (Dec. 2004), pp. 606–607. DOI: 10.1002/pamm.200410284.
- [10] K. Ehrhardt and M. C. Steinbach. “Nonlinear Optimization in Gas Networks.” In: *Modeling, Simulation and Optimization of Complex Processes*. Ed. by H. G. Bock, E. Kostina, H. X. Phu, and R. Rannacher. Springer: Berlin, 2005, pp. 139–148. DOI: 10.1007/3-540-27170-8_11.
- [11] M. M. Feistauer. *Mathematical methods in fluid dynamics*. Pitman monographs and surveys in pure and applied mathematics. Harlow, Essex, England: Longman Scientific & Technical New York, 1993. URL: <http://opac.inria.fr/record=b1084590>.
- [12] A. Fügenschuh, B. Geißler, R. Gollmer, A. Morsi, M. E. Pfetsch, J. Rövekamp, M. Schmidt, K. Spreckelsen, and M. C. Steinbach. “Physical and technical fundamentals of gas networks.” In: *Evaluating Gas Network Capacities*. Ed. by T. Koch, B. Hiller, M. E. Pfetsch, and L. Schewe. SIAM-MOS series on Optimization. SIAM, 2015. Chap. 2, pp. 17–44. DOI: 10.1137/1.9781611973693.ch2.
- [13] B. Geißler. “Towards Globally Optimal Solutions for MINLPs by Discretization Techniques with Applications in Gas Network Optimization.” PhD thesis. Friedrich-Alexander-Universität Erlangen-Nürnberg, 2011.
- [14] B. Geißler, O. Kolb, J. Lang, G. Leugering, A. Martin, and A. Morsi. “Mixed integer linear models for the optimization of dynamical transport networks.” In: *Mathematical Methods of Operations Research* 73.3 (2011), pp. 339–362. DOI: 10.1007/s00186-011-0354-5.
- [15] B. Geißler, A. Martin, A. Morsi, and L. Schewe. “The MILP-relaxation approach.” In: *Evaluating Gas Network Capacities*. SIAM-MOS series on Optimization. SIAM, 2015. Chap. 6, pp. 103–122. DOI: 10.1137/1.9781611973693.ch6.
- [16] B. Geißler, A. Martin, A. Morsi, and L. Schewe. “Using Piecewise Linear Functions for Solving MINLPs.” In: *Mixed Integer Nonlinear Programming*. Ed. by J. Lee and S. Leyffer. New York, NY: Springer New York, 2012, pp. 287–314. DOI: 10.1007/978-1-4614-1927-3_10.
- [17] B. Geißler, A. Morsi, and L. Schewe. “A New Algorithm for MINLP Applied to Gas Transport Energy Cost Minimization.” In: *Facets of Combinatorial Optimization: Festschrift for Martin Grötschel*. Ed. by M. Jünger and G. Reinelt. Berlin, Heidelberg: Springer Berlin Heidelberg, 2013, pp. 321–353. DOI: 10.1007/978-3-642-38189-8_14.
- [18] B. Geißler, A. Morsi, L. Schewe, and M. Schmidt. *Solving Highly Detailed Gas Transport MINLPs: Block Separability and Penalty Alternating Direction Methods*. Tech. rep. July 2016. URL: http://www.optimization-online.org/DB_HTML/2016/06/5523.html.
- [19] B. Geißler, A. Morsi, L. Schewe, and M. Schmidt. “Solving power-constrained gas transportation problems using an MIP-based alternating direction method.” In: *Computers & Chemical Engineering* 82 (2015), pp. 303–317. DOI: 10.1016/j.compchemeng.2015.07.005.
- [20] Z. Gu, E. Rothberg, and R. Bixby. *Gurobi Optimizer Reference Manual, Version 6.5.0*. Houston, Texas, USA: Gurobi Optimization Inc., 2015.

- [21] M. Gugat, M. Herty, and V. Schleper. “Flow control in gas networks: Exact controllability to a given demand.” In: *Mathematical Methods in the Applied Sciences* 34.7 (2011), pp. 745–757. DOI: 10.1002/mma.1394.
- [22] M. Gugat. “Boundary Controllability between Sub- and Supercritical Flow.” In: *SIAM J. Control Optim.* 42 (2003), pp. 1056–1070.
- [23] M. Gugat, F. M. Hante, M. Hirsch-Dick, and G. Leugering. “Stationary states in gas networks.” In: *Networks and Heterogeneous Media* 10.2 (2015), pp. 295–320. DOI: 10.3934/nhm.2015.10.295.
- [24] F. M. Hante, G. Leugering, A. Martin, L. Schewe, and M. Schmidt. “Challenges in optimal control problems for gas and fluid flow in networks of pipes and canals: From modeling to industrial applications.” In: *Industrial Mathematics and Complex systems: Emerging Mathematical Models, Methods and Algorithms*. Ed. by P. Manchanda, R. Lozi, and A. H. Siddiqi. Industrial and Applied Mathematics. Jan. 2017. URL: <https://opus4.kobv.de/opus4-trr154/files/121/isiam-paper.pdf>. Accepted.
- [25] M. Herty, C. Kirchner, and A. Klar. “Instantaneous control for traffic flow.” In: *Mathematical Methods in the Applied Sciences* 30.2 (2007), pp. 153–169. DOI: 10.1002/mma.779.
- [26] M. Hinze. “Optimal and instantaneous control of the instationary Navier-Stokes equations.” Technische Universität Dresden, 2002. URL: https://www.math.uni-hamburg.de/home/hinze/Psfiles/habil_mod.pdf.
- [27] R. Hundhammer and G. Leugering. “Instantaneous Control of Vibrating String Networks.” In: *Online Optimization of Large Scale Systems*. Ed. by M. Grötschel, S. O. Krumke, and J. Rambau. Berlin, Heidelberg: Springer Berlin Heidelberg, 2001, pp. 229–249. DOI: 10.1007/978-3-662-04331-8_15.
- [28] T. Koch, B. Hiller, M. E. Pfetsch, and L. Schewe. *Evaluating Gas Network Capacities*. SIAM-MOS series on Optimization. SIAM, 2015. xvii + 364. DOI: 10.1137/1.9781611973693.
- [29] T. Koch, B. Hiller, M. E. Pfetsch, and L. Schewe, eds. *Evaluating Gas Network Capacities*. SIAM-MOS series on Optimization. SIAM, 2015. xvii + 364. DOI: 10.1137/1.9781611973693.
- [30] J. E. Lagnese, G. Leugering, and E. J. P. G. Schmidt. *Modeling, Analysis and Control of Dynamic Elastic Multi-Link Structures*. Birkhäuser Boston, 1994. DOI: 10.1007/978-1-4612-0273-8.
- [31] *LaMaTTO++: A Framework for Modeling and Solving Mixed-Integer Non-linear Programming Problems on Networks*. <http://www.mso.math.fau.de/edom/projects/lamatto.html>. 2017.
- [32] M. V. Lurie. *Modeling of Oil Product and Gas Pipeline Transportation*. Wiley-VCH, 2008.
- [33] D. Mahlke, A. Martin, and S. Moritz. “A mixed integer approach for time-dependent gas network optimization.” In: *Optimization Methods and Software* 25.4 (2010), pp. 625–644. DOI: 10.1080/10556780903270886.
- [34] D. Mahlke, A. Martin, and S. Moritz. “A simulated annealing algorithm for transient optimization in gas networks.” In: *Mathematical Methods of Operations Research* 66 (2007), pp. 99–116. DOI: 10.1007/s00186-006-0142-9.
- [35] A. Martin and M. Möller. “Cutting Planes for the Optimisation of Gas Networks.” In: *Modeling, Simulation and Optimization of Complex Processes*. Ed. by H. G. Bock, E. Kostina, H. X. Phu, and R. R. Heidelberg: Springer, 2005, pp. 307–330. DOI: 10.1007/3-540-27170-8_24.

- [36] A. Martin, M. Möller, and S. Moritz. “Mixed Integer Models for the Stationary Case of Gas Network Optimization.” In: *Mathematical Programming* 105.2 (2006), pp. 563–582. DOI: 10.1007/s10107-005-0665-5.
- [37] A. Morsi. “Solving MINLPs on Loosely-Coupled Networks with Applications in Water and Gas Network Optimization.” PhD thesis. Friedrich-Alexander-Universität Erlangen-Nürnberg, 2013.
- [38] A. J. Osiadacz. *Different Transient Flow Models - Limitations, Advantages, and Disadvantages*. PSIG report 9606. Pipeline Simulation Interest Group, 1996. URL: <https://www.onepetro.org/conference-paper/PSIG-9606>.
- [39] M. E. Pfetsch, A. Fügenschuh, B. Geißler, N. Geißler, R. Gollmer, B. Hiller, J. Humpola, T. Koch, T. Lehmann, A. Martin, A. Morsi, J. Rövekamp, L. Schewe, M. Schmidt, R. Schultz, R. Schwarz, J. Schweiger, C. Stangl, M. C. Steinbach, S. Vigerske, and B. M. Willert. “Validation of nominations in gas network optimization: models, methods, and solutions.” In: *Optimization Methods and Software* 30.1 (2015), pp. 15–53. DOI: 10.1080/10556788.2014.888426.
- [40] R. Z. Ríos-Mercado and C. Borraz-Sánchez. “Optimization problems in natural gas transportation systems: A state-of-the-art review.” In: *Applied Energy* 147 (2015), pp. 536–555. DOI: 10.1016/j.apenergy.2015.03.017.
- [41] M. Schmidt. “A Generic Interior-Point Framework for Nonsmooth and Complementarity Constrained Nonlinear Optimization.” PhD thesis. Leibniz Universität Hannover, 2013.
- [42] M. Schmidt. “An interior-point method for nonlinear optimization problems with locatable and separable nonsmoothness.” In: *EURO J. Comput. Optim.* 3.4 (Nov. 2015). Online first: 09 June 2015, pp. 309–348. DOI: 10.1007/s13675-015-0039-6.
- [43] M. Schmidt, M. C. Steinbach, and B. M. Willert. “A Primal Heuristic for Nonsmooth Mixed Integer Nonlinear Optimization.” In: *Facets of Combinatorial Optimization*. Ed. by M. Jünger and G. Reinelt. Berlin, Heidelberg: Springer, 2013, pp. 295–320. DOI: 10.1007/978-3-642-38189-8_13.
- [44] M. Schmidt, M. C. Steinbach, and B. M. Willert. “An MPEC based heuristic.” In: *Evaluating Gas Network Capacities*. Ed. by T. Koch, B. Hiller, M. E. Pfetsch, and L. Schewe. SIAM-MOS series on Optimization. SIAM, 2015. Chap. 9, pp. 163–180. DOI: 10.1137/1.9781611973693.ch9.
- [45] M. Schmidt, M. C. Steinbach, and B. M. Willert. “High detail stationary optimization models for gas networks.” In: *Optimization and Engineering* 16.1 (2015), pp. 131–164. DOI: 10.1007/s11081-014-9246-x.
- [46] M. Schmidt, M. C. Steinbach, and B. M. Willert. “High detail stationary optimization models for gas networks: validation and results.” In: *Optimization and Engineering* 17.2 (2016), pp. 437–472. DOI: 10.1007/s11081-015-9300-3.
- [47] M. C. Steinbach. “On PDE Solution in Transient Optimization of Gas Networks.” In: *J. Comput. Appl. Math.* 203.2 (June 2007), pp. 345–361. DOI: 10.1016/j.cam.2006.04.018.
- [48] A. Zlotnik, M. Chertkov, and S. Backhaus. “Optimal control of transient flow in natural gas networks.” In: *2015 54th IEEE Conference on Decision and Control (CDC)*. Dec. 2015, pp. 4563–4570. DOI: 10.1109/CDC.2015.7402932.

¹FRIEDRICH-ALEXANDER-UNIVERSITÄT ERLANGEN-NÜRNBERG (FAU), LEHRSTUHL FÜR ANGEWANDTE MATHEMATIK 2, CAUERSTR. 11, 91058 ERLANGEN, GERMANY, ²FRIEDRICH-ALEXANDER-UNIVERSITÄT ERLANGEN-NÜRNBERG (FAU), DISCRETE OPTIMIZATION, CAUERSTR. 11, 91058 ERLANGEN, GERMANY, ³ENERGIE CAMPUS NÜRNBERG, FÜRTH STR. 250, 90429 NÜRNBERG, GERMANY